



**HAL**  
open science

## Experimental analysis of Pressed Adobe Blocks reinforced with Hibiscus cannabinus fibers

Younoussa Millogo, Jean-Claude Morel, Jean-Emmanuel Aubert, Khosrow Ghavami

► **To cite this version:**

Younoussa Millogo, Jean-Claude Morel, Jean-Emmanuel Aubert, Khosrow Ghavami. Experimental analysis of Pressed Adobe Blocks reinforced with Hibiscus cannabinus fibers. *Construction and Building Materials*, 2014, 52, pp.71–78. 10.1016/j.conbuildmat.2013.10.094 . hal-01850750

**HAL Id: hal-01850750**

**<https://hal.insa-toulouse.fr/hal-01850750>**

Submitted on 13 Jun 2019

**HAL** is a multi-disciplinary open access archive for the deposit and dissemination of scientific research documents, whether they are published or not. The documents may come from teaching and research institutions in France or abroad, or from public or private research centers.

L'archive ouverte pluridisciplinaire **HAL**, est destinée au dépôt et à la diffusion de documents scientifiques de niveau recherche, publiés ou non, émanant des établissements d'enseignement et de recherche français ou étrangers, des laboratoires publics ou privés.

# Experimental analysis of Pressed Adobe Blocks reinforced with Hibiscus cannabinus fibers

Millogo , Y. , Morel, J. C. , Aubert, J. E. and Ghavami, K.

**Author post-print (accepted) deposited in CURVE February 2016**

**Original citation & hyperlink:**

Millogo , Y. , Morel, J. C. , Aubert, J. E. and Ghavami, K. (2013) Experimental analysis of Pressed Adobe Blocks reinforced with Hibiscus cannabinus fibers. Construction and Building Materials, volume 52 : 71-78

<http://dx.doi.org/10.1016/j.conbuildmat.2013.10.094>

ISSN 0950-0618

DOI 10.1016/j.conbuildmat.2013.10.094

**Copyright © and Moral Rights are retained by the author(s) and/ or other copyright owners. A copy can be downloaded for personal non-commercial research or study, without prior permission or charge. This item cannot be reproduced or quoted extensively from without first obtaining permission in writing from the copyright holder(s). The content must not be changed in any way or sold commercially in any format or medium without the formal permission of the copyright holders.**

**This document is the author's post-print version, incorporating any revisions agreed during the peer-review process. Some differences between the published version and this version may remain and you are advised to consult the published version if you wish to cite from it.**

## **Experimental analysis of pressed adobe blocks reinforced with *Hibiscus Cannabinus* fibres**

Younoussa Millogo<sup>a,b\*</sup>, Jean-Claude Morel<sup>b</sup>, Jean-Emmanuel Aubert<sup>c</sup>,  
Khosrow Ghavami<sup>d</sup>

<sup>a</sup> *Unité de Formation et de Recherche en Sciences et Techniques, Université Polytechnique de Bobo-Dioulasso, 01 BP 1091 Bobo 01, Burkina Faso.*

<sup>b</sup> *LGCB, Ecole Nationale des Travaux Publics de l'Etat, LTDS UMR 5513, Université de Lyon, Rue Maurice Audin, 69518 Vaulx en Velin cedex, France*

<sup>c</sup> *Université de Toulouse, UPS, INSA, LMDC (Laboratoire Matériaux et Durabilité des Constructions), 135 Avenue de Rangueil, F-31 077 Toulouse cedex 4, France*

<sup>d</sup> *Pontificia Universidade Catolica (PUC-Rio), Rua Marques de Sao Vicente 225, 22451-041 Rio de Janeiro, Brasil*

### **Abstract**

There is an on-going search for less polluting materials and technologies, which consume little energy in their production, construction and/or utilization. Nowadays, the attention of the researchers turns to materials which were used in engineering in pre-industrial times amongst them the local vegetable fibres and earth composites are the promising materials. This paper presents the results of research on the physical and mechanical properties of Hibiscus Cannabinus Fibres which have been used in the fabrication of Pressed Adobe Blocks (PABs). The PABs have been reinforced by Hibiscus cannabinus fibres with a content of 0.2 to 0.8 wt.% and a length of 3cm and 6cm. The microstructural characteristics of the PABs composites were investigated using X-ray diffraction (XRD), thermal gravimetric analyses (TGA), scanning electronic microscopy (SEM) and video microscopy. It was established that the addition with 0.2 to 0.6 wt.% of 3 cm long fibres reduced the dimensions of the pores in the PABs with the improvement of their mechanical properties. However, the addition of 0.8 wt.% of 6 cm fibres had negative effects on the compressive strength. The elaborated Pressed Adobe Blocks specimens were suitable as a building material with an acceptable thermal comfort.

---

\* Corresponding author : Unité de Formation et de Recherche en Sciences et Techniques (UFR/ST), Université Polytechnique de Bobo-Dioulasso, 01 BP 1091 Bobo 01, Burkina Faso. Tel.: +226 70 26 33 83; fax: +226 20 98 25 77.  
E-mail address: millogokadi@gmail.com (Y. Millogo).

**Keywords:** *Hibiscus cannabinus* fibres; Pressed Adobes Blocks; Microstructural characteristics; Physical and Mechanical Characteristics, Sustainable building material.

## 1. Introduction

During the past three decades, there has been increasing interest in the research and development of nonconventional materials and technologies (NOCMATs), such as soil as a building material, bamboo and vegetable fibres, as ecofriendly materials in a wide range of applications in civil engineering and construction. Soil has been used in the construction of shelters and houses for thousands of years. At present, approximately 30% of the world's population still lives in earthen structures [1, 2]. In most developing countries, houses are essentially constructed using locally produced adobes. The binder of this material is mainly composed by the clayey fraction of the soil. Although the traditional application of adobe by local builders goes back thousands of years, their know-how has not been registered systematically in order to be transferred to future generations. As an example of a negative aspect of using adobe, at present, is its low mechanical strength in the humid state. Therefore, problems can arise during the rainy period of the year. In most part of the world before the introduction of industrial materials, such as steel and concrete, adobe was the most commonly used material for the construction of houses. In most cases adobes were stabilized by locally available vegetable fibres. This empirical practice improved the mechanical characteristics and the impermeability of adobes in different weather conditions. At the universities around the world, the emphasis of the research and development programs up to present time has been directed principally to the study of industrialized materials, and ,not the locally developed traditional materials and technologies which have been used since the beginning of the human civilization, therefore their use is now very limited.

To improve the mechanical strength, impermeability and the durability of locally produced adobe, in general, small amounts of quicklime or natural fibres are added to the soil matrix [2-18]. The use of local natural fibres, especially in developing countries, is more beneficial for

the population as fibres are locally available in abundance and their productions are of low cost and low consuming energy besides are not polluting. In the available literature, several experimental investigations have established the positive effects of the addition of vegetable fibres such as sisal, coconut, wheat straws, oil palm empty fruit bunches, jute, flax , barely straw, bamboo, cane, and lechuguilla on the physical and mechanical properties of soil composite blocks and PABs [2, 4, 6, 7, 10, 15-19] .The effect of synthetic fibres on soil composites have been also studied theoretically [20-23] with the objective of producing specific analytical model for soil composites[24,25]. The main parameters which influences strongly the physical, mechanical and the durability behavior of soil composites are: the type, tensile strength and durability of fibres besides the fibres' length and their volume fraction in the composite mix [26].

The type of fibre has an important influence on the impermeability of the composites depending on the percentage of the lignin in the fibre. Higher the percentage of lignin in the vegetable fibre higher the impermeability. Depending on the mixture of soil its differential shrinkage during the drying process could be high. To prevent the shrinkage cracks of the soil matrix fibres are added. The higher the resistance of fibres with high bonds less shrinkage cracks in the PABs. The optimum volume fractions and length for most vegetable fibres have been found to be between 0.3 percent and 0.8 percent in weight with 3cm to 8cm length respectively. Fibres tensile strength directly determines the crack resistance of fibre-reinforced soil. The long-term stability of this feature is not studied in this article, but existing buildings where fibres did not decompose in the soil validate the durability of soil composite reinforced with vegetable fibres. The fibre length determines the pullout resistance of the embedded fibre in the soil matrix and therefore directly determines the reinforcement force, which is less than or equal to the fibre tensile strength. The amount of fibre determines the intensity of the reinforcement: For small amounts (<0.2wt.%), the strength of the

reinforcement increases with the number of fibres. However, at a higher fibre mass fraction over a certain threshold, the fibres are so numerous that they weaken the soil matrix and thus lead to a lower resistance of the reinforced soil composites.

This paper presents the results of an investigation on the physical and mechanical properties of Pressed Adobe Blocks (PABs) with and without the addition of *Hibiscus cannabinus* fibres available in abundance in Burkina Faso in West Africa.

To manufacture PABs, the raw soil sample was sieved to obtain particles with a size less than 5 mm. The soil composite was mixed for 15 min until it became a homogeneous paste with water content around 20 % depending on mixture composition. The different pastes were introduced in the parallelepiped mold (295x140x100 mm<sup>3</sup>) of a GEO 50 manual press to produce the compressed soil blocks.

Pressed Adobe Blocks (PABs) were reinforced with 0.2 to 0.8 wt.% of 3 cm and 6 cm length fibres. The bonding of the fibres in the composite was studied through the microstructural characteristics of the PABs composite using scanning electronic microscopy (SEM) and video microscopy.

## **2. Materials and experimental procedures**

### **2. 1. Clayey soil sample**

#### **2. 1. 1. Soil properties**

The clayey soil from Rochechinard, at a site located in the Isère valley (France) was chosen for this investigation. It is a red lateritic soil. The particle size distribution presented in **Fig. 1** was determined by wet sieving and sedimentation. It was mainly composed of 45wt.% sand, 30wt.% silt and 25wt.% clay (particle size <2 µm). The Atterberg limits of the sample was: liquid limit ( $w_L = 38\%$ ), plastic limit ( $w_P = 20\%$ ) and plasticity index ( $PI = 18\%$ ). The

methylene blue value and the activity of clay minerals were, respectively, 2.5 g/100 g and 10 g/100 g.

### **2. 1.2. Mineralogical characterization**

X-ray diffraction was performed on a crushed sample of the size <80 μm using a Siemens D5000 power X-ray diffractometer equipped with a monochromator using a Ka ( $\lambda = 1.789 \text{ \AA}$ ) cobalt anticathode. Thermal Gravimetric Analyses (TGAs) on the crushed samples heated up to 950°C at a constant rate of 10°C/min were carried out to establish the thermal mineralogical characterization of the soil.

### **2. 1.3. Chemical composition**

The major oxide composition was estimated on the basis of the macroelemental analysis performed on digested crushed samples of the size <80 μm by inductively coupled plasma–atomic emission spectrometry (ICP-AES). The loss upon ignition and calcinations at 1000°C was also measured.

### **2. 1.4. Mineralogical composition**

The mineralogical composition of the sample was obtained by using the results of X-ray diffraction and the chemical analyses. Relation 1 was used to calculate the amount T (a) in oxide (wt. %) of chemical element « a » :

$$T(a) = \sum M_i P_i(a) \quad (1):$$

where:

$M_i$  = amount (in wt.%) in mineral  $i$  in the material under study containing the element  $i$  ;

$P_i(a)$  = proportion of element  $a$  in the mineral  $i$ .

### **2.1.5. Microscopic observations**

For scanning electron microscopy (SEM) observations, a JEOL 6380 LV equipped with a backscattered electron (BSE) detector was used. The microscopic examinations were carried

out on the fractured surfaces of the PAB pieces obtained after flexural strength testing. Direct observations were made using SEM in low-vacuum (LV) mode (no metallization necessary, with a pressure of 60 Pa in the SEM chamber). The images of these fractured surfaces were taken with a video microscope directly on the fresh fractured surface.

## **2.2. *Hibiscus cannabinus* fibres**

*Hibiscus cannabinus* is a plant in the *Malvaceae* family. It is an annual herbaceous plant (rarely a short-lived perennial) growing to 1.5 to 3.5 m in height with a woody base. The diameters of the stems are 1 to 2 cm, and they are often but not always branched. The leaves are 10 to 15 cm long and variable in shape. Leaves near the base of the stems are deeply lobed with 3 to 7 lobes, while leaves near the top of the stem are shallowly lobed or unlobed lances. The flowers are 8 to 15 cm in diameter and white, yellow, or purple; when white or yellow, the center is still dark purple. The fruit is a capsule 2 cm in diameter, containing several seeds. The plant was cut at the age of six months. The *Hibiscus cannabinus* plant stem and extracted fibres are presented in **Fig. 2 (a, b)**. The fibres were obtained from the stems near Bobo-Dioulasso in Burkina Faso in West Africa. The fibres were extruded manually by pulling the fibres from the stalks.

## **2.3. Experimental procedures**

### **2.3.1 Physical and mechanical characteristics of the fibres**

The diameters of the fibres were assumed of a circular form, were measured using a micrometer with a precision of 0.01 mm. The natural humidity of the air-dried fibres after being kept in an oven at 105°C for 24 h were established.

The tensile strength of fibres was established according to ASTM D 3822–07 choosing the dried samples in the laboratory with their natural moisture [27]. The 100mm gauge length test

specimens were realized at the Mechanical Testing Laboratory (ITUC) of the PUC-Rio, in the universal testing machine INSTRON Model 5500R No.6233 with the maximum load capacity of 10000kN. The data from the testing machine are analyzed using software Bluehill which is coupled to it. The test samples were fixed to the grips of the machine, removing the slack without stretching the sample; making certain that specimen is well aligned and straight within the grips and is in the line along the applied load to the fibre. Any misalignment could produce the transverse movement of the clamps and hence introducing errors in the measurements of elongation and contribute to the premature failure of the fibre. The displacement of the machine clamps was 0,05 mm/s until the failure of the fibre. The specimen fixed in the INSTRON testing machine before and after failure is shown in **Fig. 3**. For not having biased results some fibres were tested in the Laboratory of Structures and Materials (LEM) of the Civil Engineering Department of the PUC - Rio, in the EMIC DC3000 universal machine, connected to a PC computer where the data are processed using TESC program. The same procedure using ASTM D 3822–07 was followed.

### **2.3.2 Manufacturing and test procedure for the pressed adobe blocks (PABs)**

To manufacture PABs, the raw soil sample was sieved to obtain particles with a size less than 5 mm. The powdered sample was mixed with fibre lengths of 3 cm and 6 cm, up to 0.8wt.% in relation to the weight of the soil. The average water/soil ratio used was 20 wt.%. The soil composite was mixed for 15 min until it became a homogeneous paste. The different pastes were introduced in the parallelepiped mold ( $295 \times 140 \times 100 \text{ mm}^3$ ) of a GEO 50 manual press to produce the compressed soil blocks. The pressure applied during compaction was approximately 2 MPa. The as-molded PABs were dried in the laboratory at room temperature (average 22°C) with a humidity of 60% until the block weight became constant (average 3 weeks) [25].

The unconfined compressive and three-point bending strength tests were carried out using an INSTRON hydraulic press on the PAB specimens. The test was conducted at a constant speed of  $0.01 \text{ mm}\cdot\text{s}^{-1}$ . The load sensor used had a capacity of 50 kN.

The thermal conductivity ( $\lambda$ ) of the PABs was measured on PAB cut samples ( $140 \times 140 \times 100 \text{ mm}^3$ ). The measurements were made with a hot wire probe.

Laboratory tests were conducted to simulate the rain erosion process using a spray test with a flow of 5 L/min for 10 min. The spray was placed 12 cm above the PAB. To simulate the angle of impact of the rain drops, the PAB was placed at an angle of approximately  $30^\circ$  from the horizontal. The percentage of loss material after the test characterizes the erosion degree of PABs, which was estimated by an erosion coefficient in Equation 2.

$$C_E(\%) = \frac{M_0 - M_s}{M_0} * 100 \quad (2)$$

in which  $M_0$  is the weight of the air-dried PAB and  $M_s$  is the weight of the PAB submitted to the erosion test and dried at  $105^\circ\text{C}$  for 24 h.

The abrasion strength test was carried out on the PAB submitted to mechanical erosion by using a metal brush with a constant pressure over a given number of cycles. The friction was applied to the PAB faces that would be exposed in situ. The coefficient of abrasion expresses the ratio of the quantity of material detached and the surface by brushing, which is given in Equation 3.

$$C_A (\text{g}/\text{cm}^2) = \frac{m_1 - m_2}{S} \quad (3)$$

in which  $S$  is the brushed surface and  $m_1$  and  $m_2$  are the masses before and after brushing. The difference is proportional to the abrasion. The test was realized according to the procedure developed in [27].

### 3. Results and discussion

#### 3.1. Physical, mechanical and chemical characteristics of the fibres

The physical properties of the fibres (diameter, natural humidity, specific weight and, water absorption) are shown in **Table 1**. The diameters and the specific weights of *Hibiscus cannabinus* fibres were in the range of the values for sisal, coconut and lechuguilla fibres [4, 16], but these parameters were smaller than those reported for straw fibres and oil palm empty fruit bunch fibres [10, 17]. The natural humidity of the fibres was inferior, but their water absorption was superior to that of sisal, coconut and lechuguilla fibres [4, 16]. Straw fibres presented higher water absorption, with value 500%-600% higher than *Hibiscus cannabinus* fibres [10]. The tensile strength of *Hibiscus cannabinus* fibres was higher than the tensile strength of sisal, lechuguilla, coconut and oil palm empty fruit bunch fibres [4, 16, 17].

The tensile stress-strain curves are given in the **Fig. 4**. The **Table 2** shows the physical properties of samples and the modulus of elasticity (E) that was calculated by drawing a line tangent to the stress-strain curve. Considering all the values obtained, average modulus of elasticity are 136 GPa, with a standard deviation of 25 GPa and the coefficient of variation is 19%.

The tensile strength has a mean value of 1 GPa, with a high Standard Deviation depending on the natural variability of the fibres. The tensile stress is approximately twice higher than steel with a stiffness twice smaller, which means that this material is 4 times more deformable than steel. This deformability is favorable to reinforce PAB which is a material with a low stiffness [25].

#### 3.2. Mineralogical and chemical characterizations of the soil

The powder X-ray diffraction pattern of the soil sample is shown in **Fig. 5**. The X-ray diffraction showed that the sample was essentially composed of quartz ( $\text{SiO}_2$ ), kaolinite ( $(2\text{SiO}_2 \cdot \text{Al}_2\text{O}_3 \cdot 2\text{H}_2\text{O})$ ), illite ( $(\text{K Al}_2 (\text{Al Si}_3)\text{O}_{10}(\text{OH})_2)$ ), goethite ( $\text{Fe}_2\text{O}_3 \cdot \text{H}_2\text{O}$ ) and a small amount of calcite ( $\text{CaCO}_3$ ).

To complete the mineralogical characterization and identify the amorphous compounds, the sample was subjected to thermal gravimetric analyses (TGAs). The results

are presented in **Fig. 6**. The loss of mass around 120°C is due to the hygroscopic water. The thermal phenomena around 275, 500 and 700°C characterized the dehydroxylation of goethite, the kaolinite transformation into metakaolinite and the decomposition of calcite and its transformation into lime with the loss of carbon dioxide, respectively.

The chemical composition of the raw material is given in **Table 3**. The chemical composition showed a high amount of silica and alumina, a low quantity of iron oxide, calcium oxide and potassium oxide. These results were well corroborated by the identified mineral phases. Based on the chemical composition and the minerals identified by X-ray diffraction, the mineralogical composition was estimated using Equation 1. The sample was composed of kaolinite (45 wt.%), quartz (23 wt.%), illite (14 wt.%), goethite (7 wt.%) and calcite (4 wt.%).

### **3.3. Microscopic observations**

Scanning electronic microscopy micrographs of the fractured surfaces of the PABs are presented in **Fig. 7 (a-d)**. The micrograph of the PAB without fibres is shown in **Fig. 7-a**; a heterogeneous microscopy with some cracks and large pores can be observed. The PAB reinforced with 0.2 wt.% of 3 cm fibres showed homogeneous microstructure, as can be observed in **Fig. 7-b**, with small size pores and no cracks. When the fibre content increased to 0.4 wt.% of 3 cm length fibres, the PAB microscopy (**Fig.7-c**) was more homogeneous. The rough surface and the warp of the fibres improved the link between the soil grains. In the case of a higher fibre content of 0.8 wt.% of 3 cm length fibres, the fibres were distributed in the bulk (**Fig. 7d**).

Video microscope images of the fractured surfaces of PABs are shown in **Fig. 8 (a-d)**. The image of an unreinforced PAB (**Fig.8-a**) showed the heterogeneity of the structure and the presence of large pores, often disconnected particles and significant fractured areas. The

presence of larger pores explains the lower compactness of the structure. With fibres reinforcing the PAB (**Fig. 8 b-d**), the soil matrix became more compact, enhancing the connection between soil grains. The fibres with a rough aspect seem well distributed in the soil matrix and adhered well to the soil.

### **3.4. Physical and mechanical properties of the PAB**

The evolution of the thermal conductivity ( $\lambda$ ) versus the fibre content and fibre length is presented in **Fig. 9**. The thermal conductivity decreased with increasing amounts and lengths of fibres. With long fibres 6 cm in length, there is a greater occupation of volume in the PAB compared with 3 cm long fibres, and the thermal conductivity decreased slightly. The decrease of the thermal conductivity is favorable for buildings because it improves energy savings. The decrease varied from 9% for 0.4 wt% of 3 cm fibres to 20% for 0.8 wt% of 6 cm fibres. On the thermal behaviour point of view, the best fibre content would be 0.8 wt% with 6cm long fibres which corresponds to the decrease of the PAB dry density due to degradation of the soil matrix due to the bulky fibres. However this fibre content and length weakens the resistance to erosion, which may not be acceptable in the case of adobes.

The results of erosion and abrasion tests are shown in **Fig. 10**. The adhesion of fibres with the clay matrix shown by SEM and by video microscopy with a reduction of pores explains this result. The PABs reinforced with 6 cm fibres were more eroded than those with shorter fibres. Even for a small amount of 3 cm fibres (0.2 and 0.4 wt.%), the improvement was obtained because of good repartitioning of the fibres in the clay matrix. With a high amount of fibres (0.8 wt.%), a small increase of the value of the erosion was observed, which can be explained by the presence of bulky fibres in the PABs, as shown by microscopic observations. Abrasion of the PABs decreased down to 0.4 wt.% and slightly increased with the length and content of the fibres. For the 0.8 wt.% fibre content with 6 cm long fibres, the abrasion was

greater than that of unreinforced PABs because of the bulky distribution of fibres in the clay matrix, as shown by microscopic observations. The abrasion coefficient explains why the fibre-reinforced PAB was resistant to mechanical erosion: fibre adhesion with the raw material matrix increased its resistance.

The compressive and flexural strength versus fibre content and fibre length are shown in **Fig. 11** and **Fig. 12**. As for erosion and abrasion, the compressive strength had an optimum value near 0.4 wt.% and then decreased. At this optimum, the compressive strength increased by 16% for short fibres (3 cm) and by 8% for long fibres (6 cm). The increase of the compressive strength is linked to the homogeneous microstructure because of the presence of fewer pores, as demonstrated by microscopic studies (SEM and video microscopy). These pores are occupied by fibres. Moreover, the microscopic observations of PABs reinforced with fibres proved the quasi-absence of cracks, which shows that the association of fibres and the clay matrix prevents the spread of cracks and contributes therefore to the improvement of the compressive strength. For long fibres and high amounts of fibres (0.8 wt.% and 6 cm), the compressive strength is smaller when compared with that of unreinforced PABs because of the degradation of the soil matrix due to the bulky fibres. The compressive strength of reinforced samples, except for the one manufactured with 0.8 wt.% 6cm fibres, are higher than other values reported in the literature on soil blocks stabilized with fibres [2, 4, 12, 13], which could be due to the high resistance of *Hibiscus cannabinus* fibres compared with those used in other studies.

The flexural strength increased and decreased for high contents of fibres. For all formulations, fibre-reinforced PABs presented flexural strength values higher than those of unreinforced PABs. The increase of this parameter is mainly due to the high tensile strength of *Hibiscus cannabinus* fibres, which was proven by microscopic observations that showed uncut fibres. Furthermore, the homogeneous repartitioning and adhesion of fibres with the

clay matrix is an additional proof of the increase of the flexural strength. The fibre length did not influence the flexural strength for fibre content of 0.4 and 0.8 wt%. However in the case of 0.2wt%, the difference is high between 3cm and 6cm fibre long. This means that the embedded length of the fibre is important in this case of low fibre content. The results obtained with *Hibiscus cannabinus* fibres were better than those reported for soil reinforced by straw and sisal [7, 10, 13]. The results of this investigation show that the fibre-stabilized PABs are acceptable as a building material according to the required standards [29].

#### 4. Conclusions

The effects of *Hibiscus cannabinus* fibres (amount: 0.2-0.8 wt.%; length: 3 and 6 cm) from Burkina Faso on the microstructural characteristics of Pressed Adobes Blocks elaborated with a clayey material from Rochechinard (France) were investigated. Additions of *Hibiscus cannabinus* fibres did not lead to the formation of new mineralogical phases but contributed a homogenous microstructure within the specimens with the reduction of the pore size. *Hibiscus cannabinus* fibre addition improved the physical and mechanical characteristics of the specimens. The impact was observed with 3-cm-long fibres. Longer fibres and high contents of fibres (6 cm; 0.8 wt.%) had a negative effect on the compressive strength. The increase of the mechanical properties is linked to the nonpropagation of cracks due of the presence of fibres in the clay matrix. The impact of these fibres on the flexural strength was positive because of the high tensile strength of the fibres and their adhesion to the clay matrix.

It is shown here that it is possible to find an optimum material thanks to the addition of fibres. This reinforced material can be optimized by modifying the quantity of fibres and their length. The optimization can be oriented through the type of building concerned, for example improving the tensile strength or reducing the thermal conductivity. If the principal problem

of adobes construction is its durability, then the resistance against erosion and abrasion must be the best as possible, which corresponds in our study to a fibre content of 0.3 to 0.5 wt% with 3cm or 6 cm long fibres.

The reinforced Pressed Adobe Block specimens were suitable for use as a building material which is very important for developing countries, particularly Burkina Faso, because of the abundance and low cost of *Hibiscus cannabinus* fibres.

### **Acknowledgements**

Funding of this project was provided by a grant from Aire-Sud Project and Région Rhône-Alpes. Erwan Hamard from ENTPE is thanked for his help in the experiments for the compression tests and Lorena Chamoro, Ricardo Andre Ph.D., students at PUC-Rio for the execution of tensile tests. Sobéré Augustin Traoré from the Université Polytechnique de Bobo-Dioulasso, Burkina Faso, for his help in *Hibiscus cannabinus* plant characterization.

## References

- [1] Goodhew S, Griffiths R. Sustainable soil walls to meet the building regulations. *Energy Build* 2005; 37: 451-459.
- [2] Binici H, Aksogan O, Shah T. Investigation of fibre reinforced mud bricks as a building material. *Construc Build Mater* 2005; 19: 313-318.
- [3] Walker PJ. Strength, durability and shrinkage characteristics of cement stabilised soil blocks. *Cem. Concr. Comp* 1995; 17: 301-310.
- [4] Ghavami K, Toledo Filho RD, Barbosa NP. Behaviour of composite soil reinforced with natural fibres. *Cem and Concr Compos* 1999; 21: 39-48.
- [5] Reddy BVV, Hubli S. Properties of lime stabilised steam- cured blocks for masonry. *Mater Struct* 2002 ; 35: 293-300.
- [6] Tolêdo Filho R D, Ghavami K, England G L, Scrivener K. Development of vegetable fibre-mortar composites of improved durability. *Cem and Concr Compos* 2003 ; 25: 185-196.
- [7] Mesbah A, Morel JC, Walker P, Ghavami K. Development of a direct tensile test for compacted soil blocks reinforced with natural fibres. *J Mater Civil Eng* 2004 ; 16(1): 95-98.
- [8] Reddy BVV, Gupta A. Characteristics of cement-soil mortars. *Mater Struct* 2005a ; 38: 639-650.
- [9] Reddy BVV, Gupta A. Characteristics of soil-cement blocks highly sandy. *Mater Struct* 2005b ; 38: 651-658.
- [10] Bouhicha M, Aouissi F, Kenai S. Performance of composite soil reinforced with barley straw. *Cem and Concr Compos* 2005; 27: 617-621.
- [11] Kumar A, Walia S B, Mohan J. Compressive strength of fibre reinforced highly compressible clay. *Construc Build Mater* 2006 ; 20 : 1063-1068.

- [12] Achenza M, Fenu L. On soil stabilization with natural polymers for soil masonry construction. *Mater Struct* 2006; 39: 21-27.
- [13] Yetgin S, Cavdar O, Cavdar A. The effects of the fibre contents on the mechanic properties of the adobes. *Construc Build Mater* 2008; 22(3): 222-227.
- [14] Millogo Y, Hajjaji M, Ouedraogo R. Microstructure and physical properties of lime-clayey adobe bricks. *Construc Build Mater* 2008 ; 22(2) : 2386-2392.
- [15] Galán-Marin C, Rivera-Gómez C, Petric J. Clay-based composite stabilized with natural polymer and fibre. *Construc Build Mater* 2010; 24: 1462-1468.
- [16] Juárez C , Guevara B, Durán-Herrera A. Mechanical properties of natural fibres reinforced sustainable masonry. *Construc Build Mater* 2010; 24: 1536-1541.
- [17] Ismail S, Yaacob Z. Properties of laterite bricks reinforced with oil palm empty fruit bunch fibres. *Pertanika J Sci & Technol* 2011 ; 19 (1) : 33-43.
- [18] Quagliarini E, Lenci S. The influence of natural stabilizers and natural fibres on the mechanical properties of ancient Roman adobe bricks. *J Cult Herit* 2010 ; 11(3): 309-314
- [19] Hejazi S.M, Sheikzadeh M, Abtahi S.M and Zadhoush A. A simple review of soil reinforcement by using natural and synthetic fibres. *Construction and Building Materials* 30 (2012) 100-116
- [20] Morel JC, Gourc JP. Behavior of sand reinforced with mesh elements. *Geosynth Int* 1997 ; 4 (5) : 481-508.
- [21] Falorca IMCFG, Pinto MIM. Effect of short, randomly distributed polypropylene microfibrils on shear strength behaviour of soils. *Geosynth Int* 2011 ; 18(1): 2-11.
- [22] Hosseinpour I, Mirmoradi SH, Barari A, Omidvar M. Numerical evaluation of sample size effect on the stress-strain behavior of geotextile-reinforced sand. *J Zhejiang Univ Sc A* 2010 ; 11(8) : 555-562.

- [23] Yilmaz Y. Experimental investigation of the strength properties of sand-clay mixtures reinforced with randomly distributed discrete polypropylene fibres. *Geosynth Int* 2009 ; 16(5): 354-363.
- [24] Morel JC, Ghavami K, Mesbah A. Theoretical and Experimental Analysis of Composite Soil Blocks Reinforced with Sisal Fibres Subjected to Shear. *Masonry Int* 2000 ; 13(2) : 54-62.
- [25] Kouakou H, Morel JC. Mechanical performance of nonindustrial building material manufactured with clay as natural binder. *Appl Clay Sci* 2009 ; 44 : 27–34.
- [26] Toledo Filho RD. Natural fibre reinforced mortar composites: experimental, characterisation. Ph.D. Thesis, DEC-PUC-Rio Brazil, 1997 . 472 pp.
- [27] ASTM D 3822 - 07. Standard Test Method for Tensile Properties of Single Textile Fibres. 2007
- [28] Boubekeur S and Rigassi V. Compressed Earth Blocks. Testing Procedures 2000 ; Série Technologies 2000, N°16.
- [29] Mbumbia L, Mertens de Wilmars A, Tirlocq J, Vandeneede V. Influence du processus de fabrication sur les propriétés des briques à base de latérite. *Sil Ind* 2000 ; 65(9-10) : 101-109.

<b>Properties</b>	<b>Results</b>
Diameter (mm)	0.13
Natural humidity: H (%)	6.10
Water absorption: W (%)	307
Specific weight : $\gamma$ (g/cm <sup>3</sup> )	1.04

**Table 1: Physical properties of *Hibiscus Cannabinus* fibres**

**Table 2 : Properties of the fibres**

<b>N°</b>	<b>Diameter (mm)</b>	<b>Area (mm<sup>2</sup>)</b>	<b>E (GPa)</b>
1	0.12	0.01	169
2	0.09	0.01	149
3	0.12	0.01	138
4	0.16	0.02	104
5	0.13	0.01	119

**Table 3: Chemical composition of the raw material**

<b>Oxides</b>	SiO <sub>2</sub>	Al <sub>2</sub> O <sub>3</sub>	Fe <sub>2</sub> O <sub>3</sub>	MgO	CaO	P <sub>2</sub> O <sub>5</sub>	MnO	Na <sub>2</sub> O	K <sub>2</sub> O	TiO <sub>2</sub>	LOI*	<b>Total</b>
<b>Wt.%</b>	50.6	23.44	5.81	1.13	2.48	0.17	0.02	0.05	1,69	0.65	14.91	100.43

\* Loss on ignition at 1000°C

### Figures Captions

**Fig. 1: Particle size distribution of the raw material**

**Fig. 2: Pictures of the *Hibiscus cannabinus* stem and its extracted fibers**

a: *Hibiscus cannabinus* plant stem; b: extracted fibers

**Fig. 3: Tensile test device adapted to the fibers**

**Fig. 4: Tensile stress-strain curves of the fibers**

**Fig. 5: X-ray diffraction pattern of the raw material**

k: kaolinite ; q: quartz ; i : illite ; g : goethite ; c : calcite

**Fig. 6: TGA and DTGA curves of the raw material**

a: TGA; b: DTGA

**Fig. 7: SEM micrographs of the raw PAB and the fiber-reinforced PAB**

a: unreinforced material; b: 0.2 wt.% fibers, 3 cm; c: 0.4 wt.% fibers, 3 cm; d: 0.4 wt.% fibers, 3 cm

**Fig. 8: Video microscope images of the raw and fiber-reinforced PABs**

a: raw material; b: 0.2 wt.% fibers, 3 cm; c: 0.4 wt.% fibers, 3 cm; d: 0.8 wt.% fibers, 3 cm

**Fig. 9: Thermal conductivity evolution with the content and the length of fibers**

**Fig. 10: Evolution of erosion and abrasion coefficients as a function of the content and**

**the length of fibers**

**Fig. 11: Compression strength of fiber-stabilized PAB**

**Fig. 12: Flexural strength of fiber-stabilized PAB**

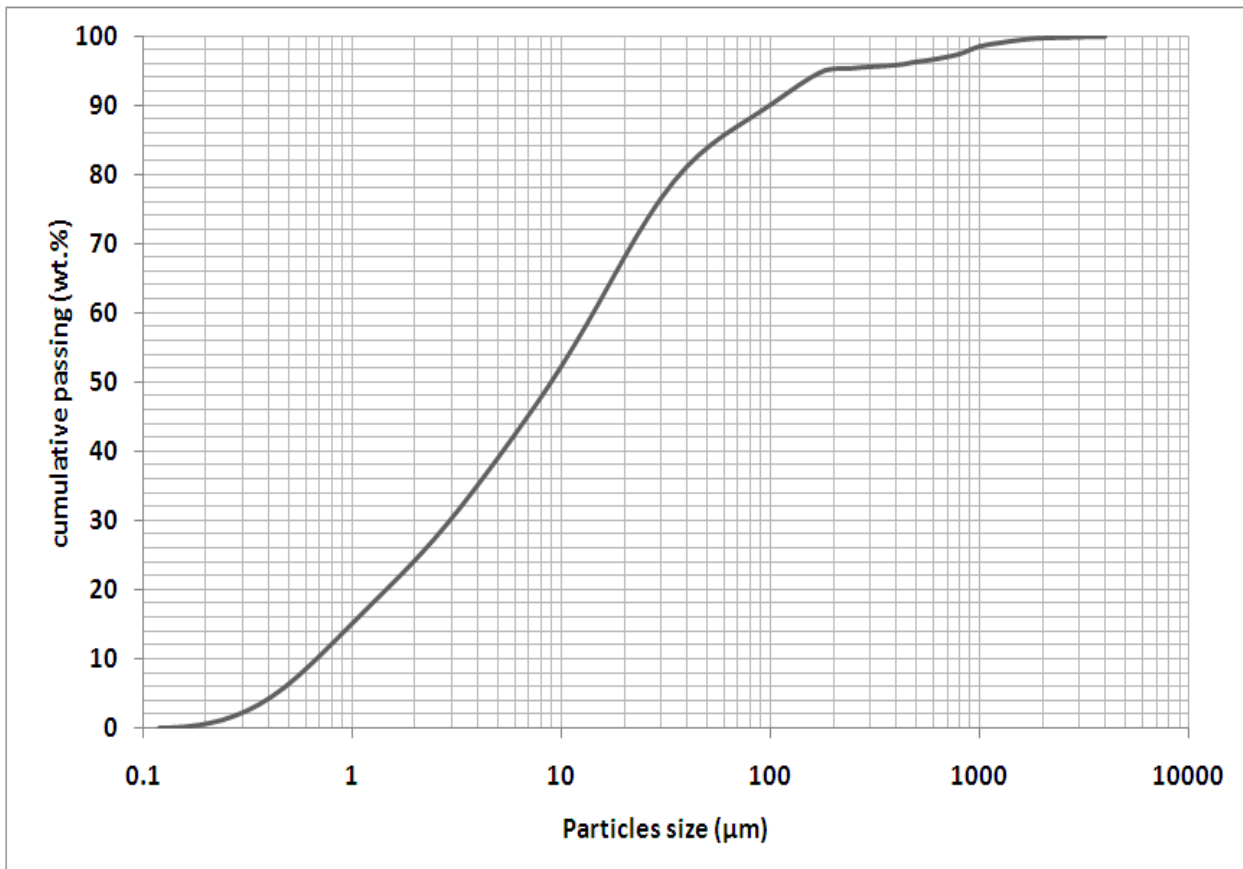


**Fig.1**



**Fig.2-a**



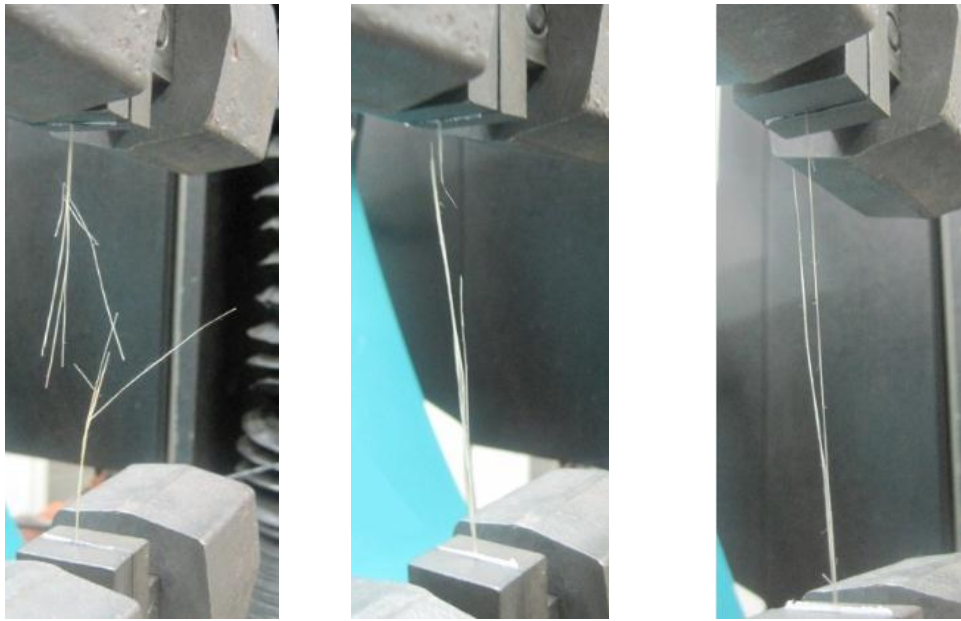


**Fig.3**



**Fig. 4.** Procedure to measure the thermal conductivity on PABs.

**Fig.4**



Figure 5

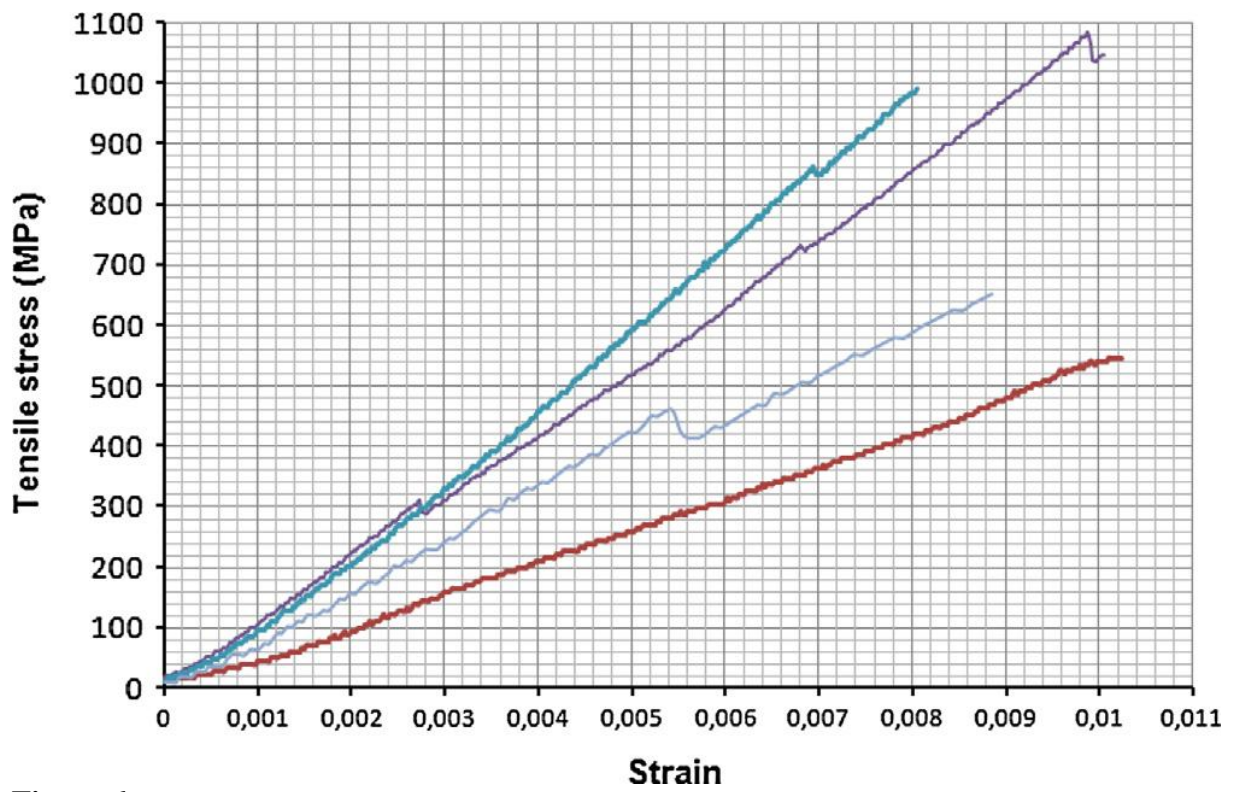
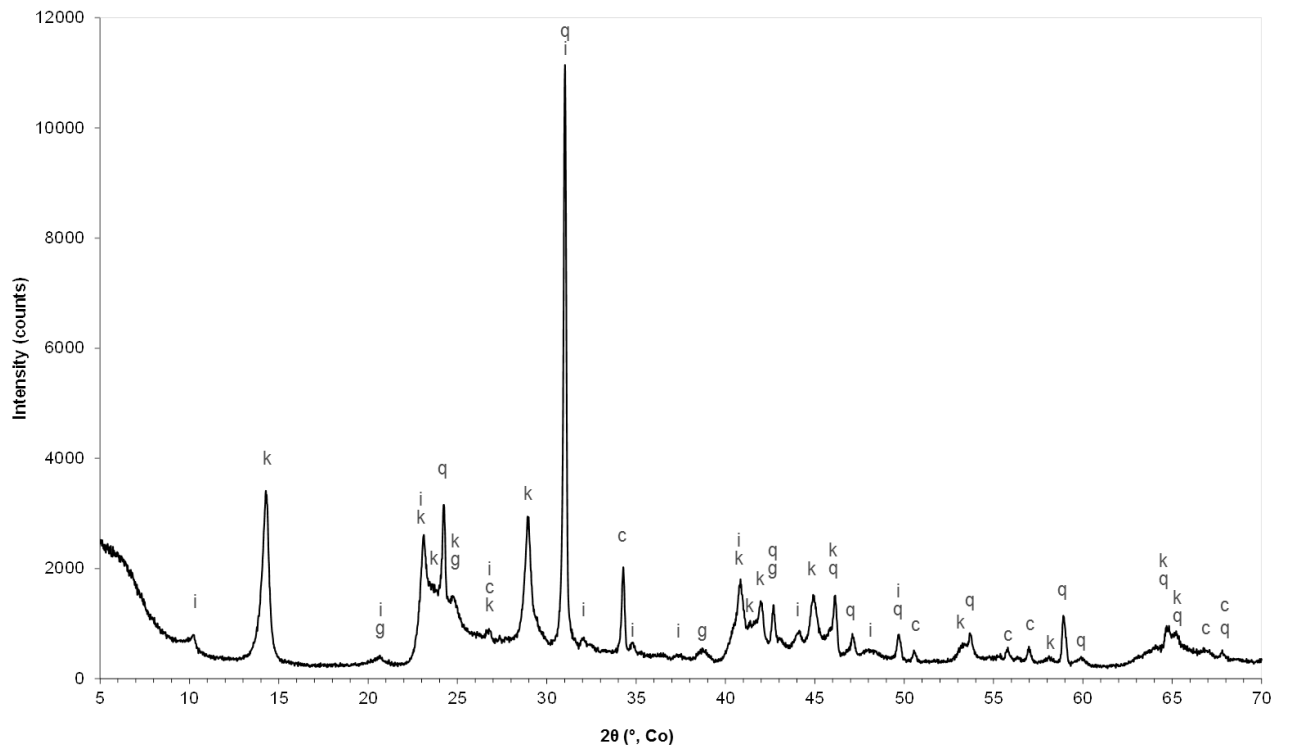
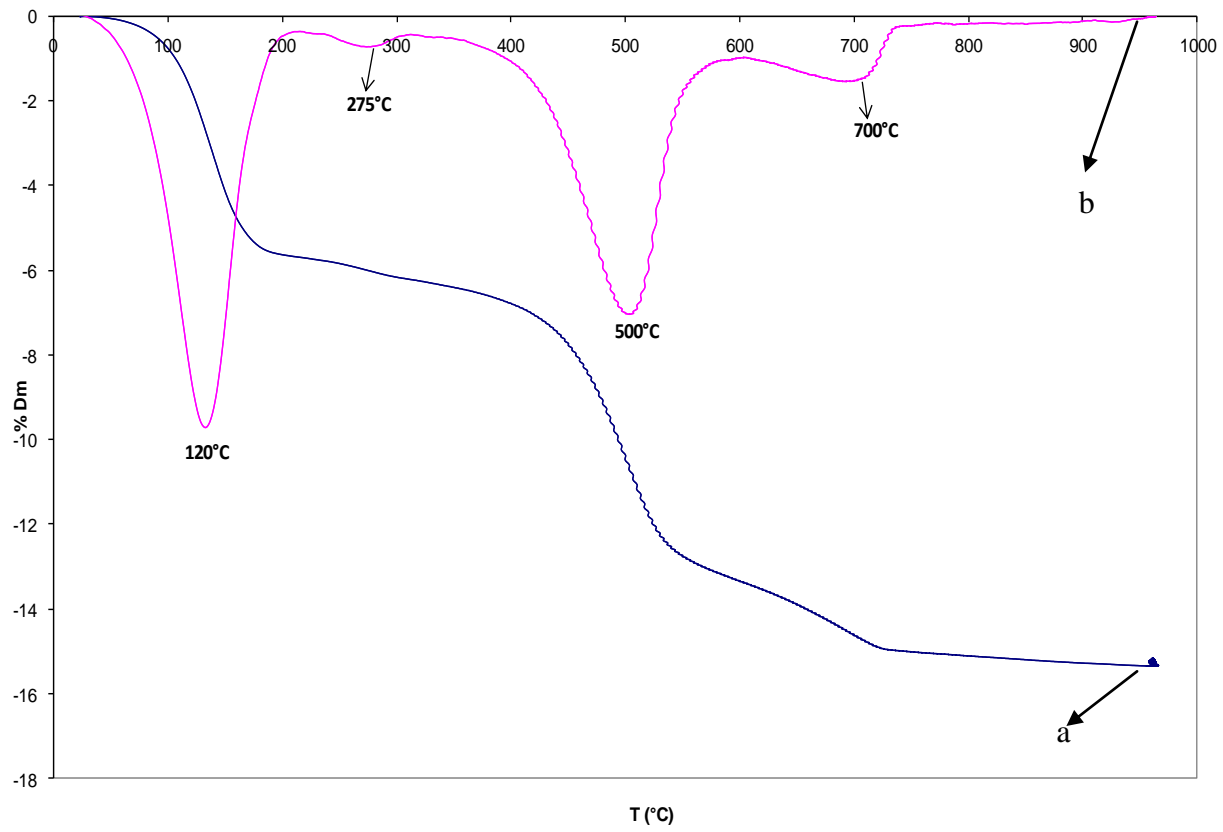


Figure 6



**Fig 7**



**Fig.8**

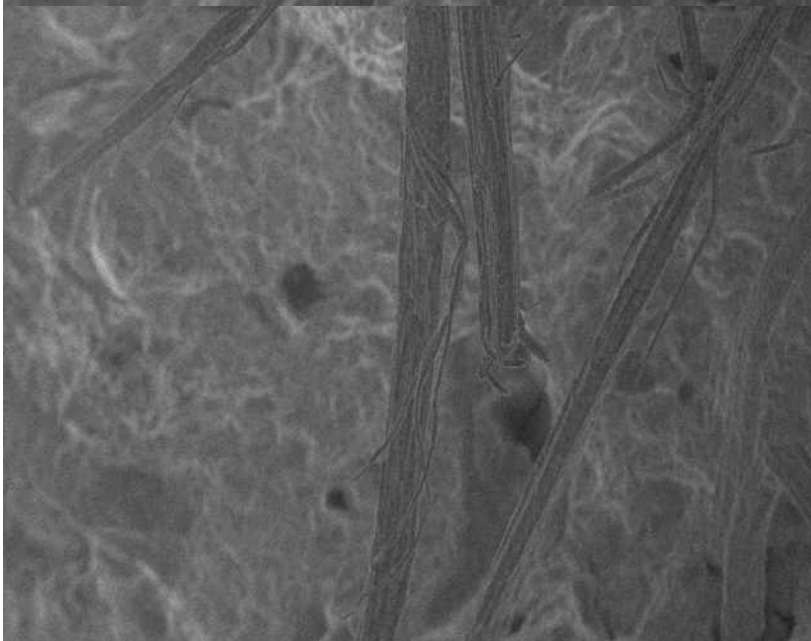
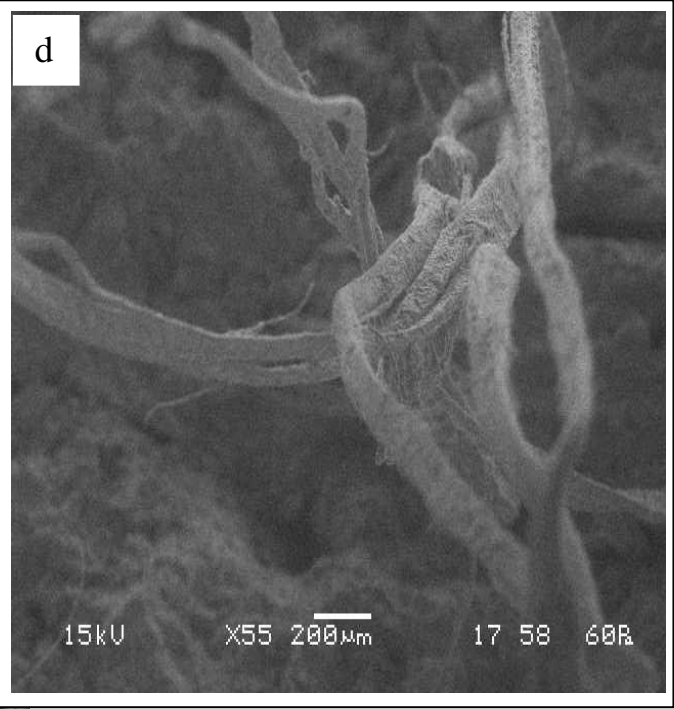
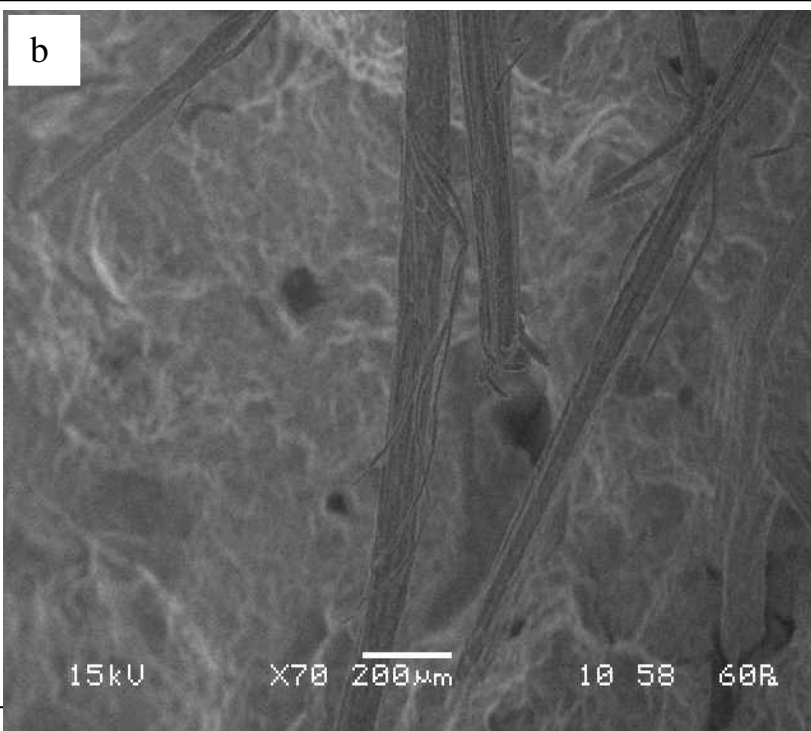
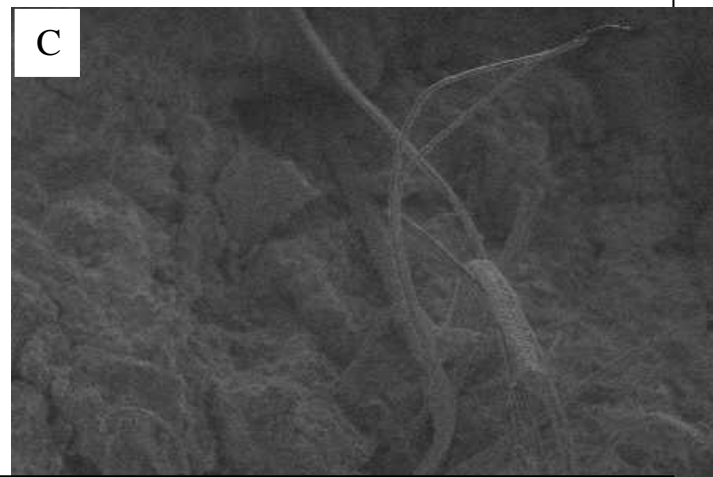
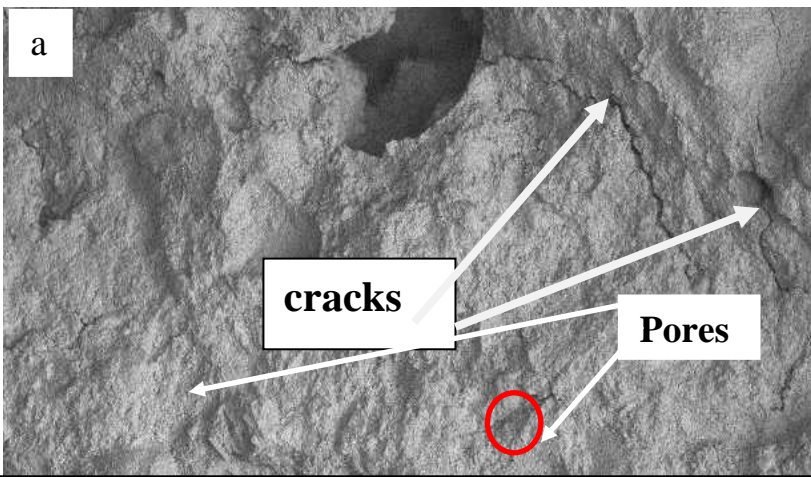




**Fig.10**

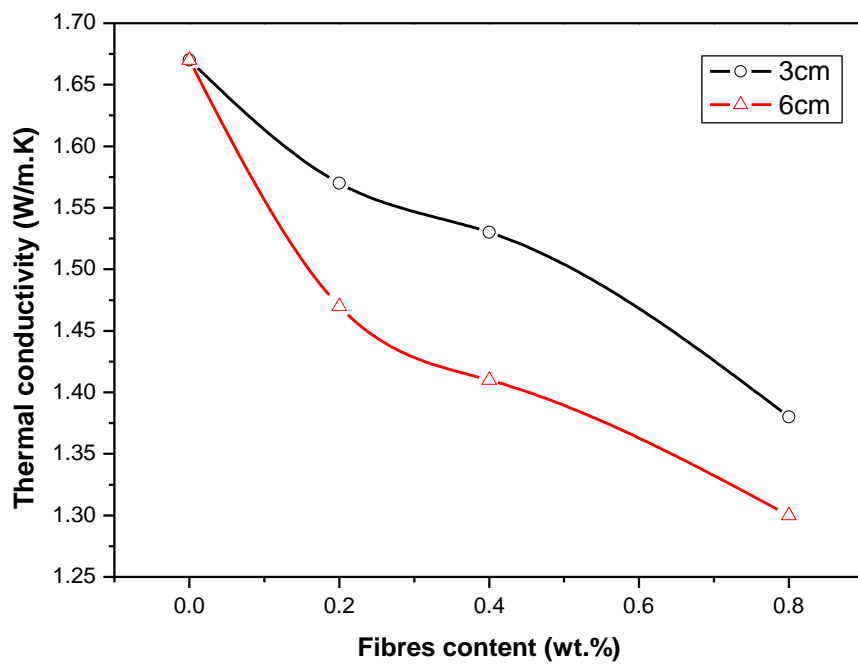


**Fig.11**

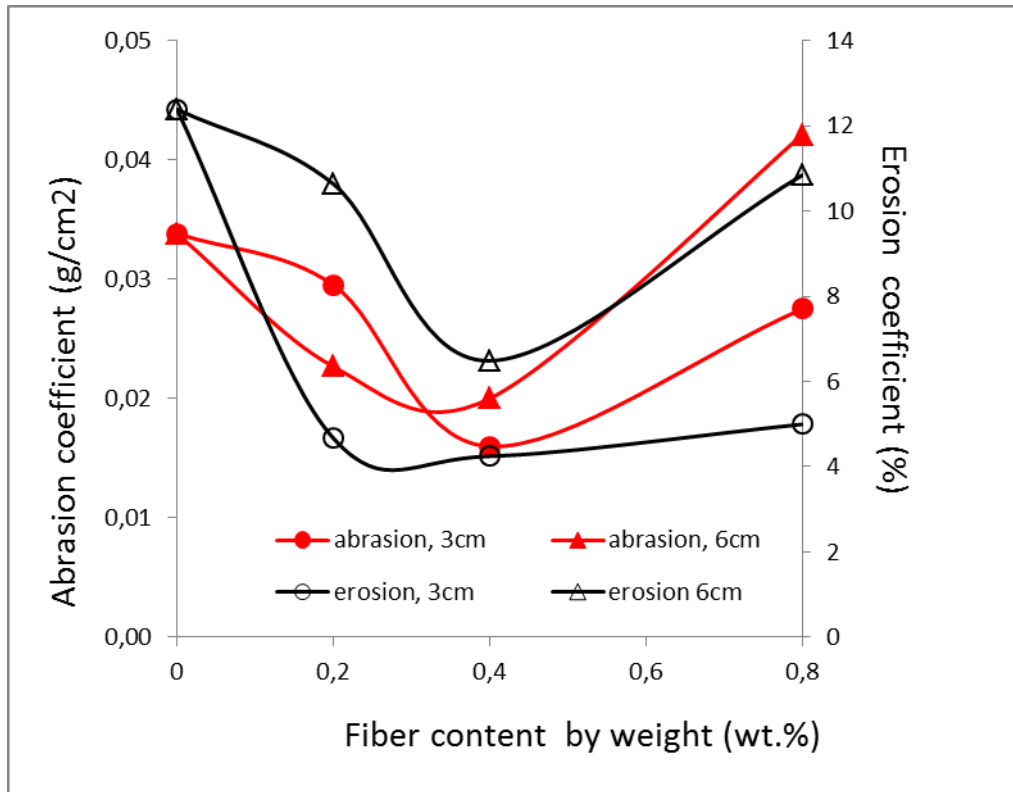


**Fig.12**

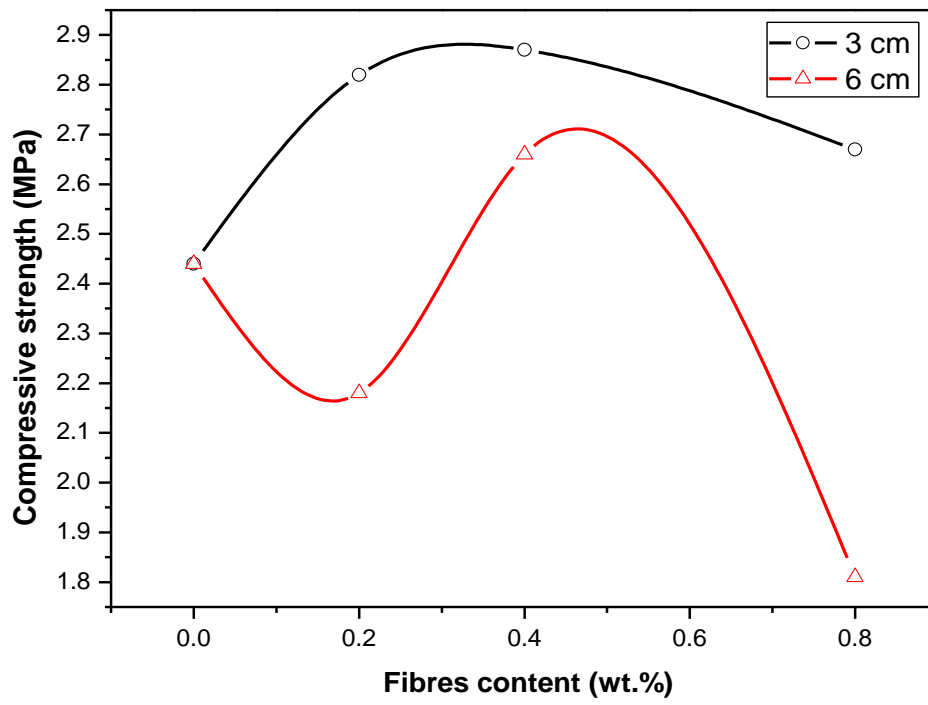


**Fig.13**

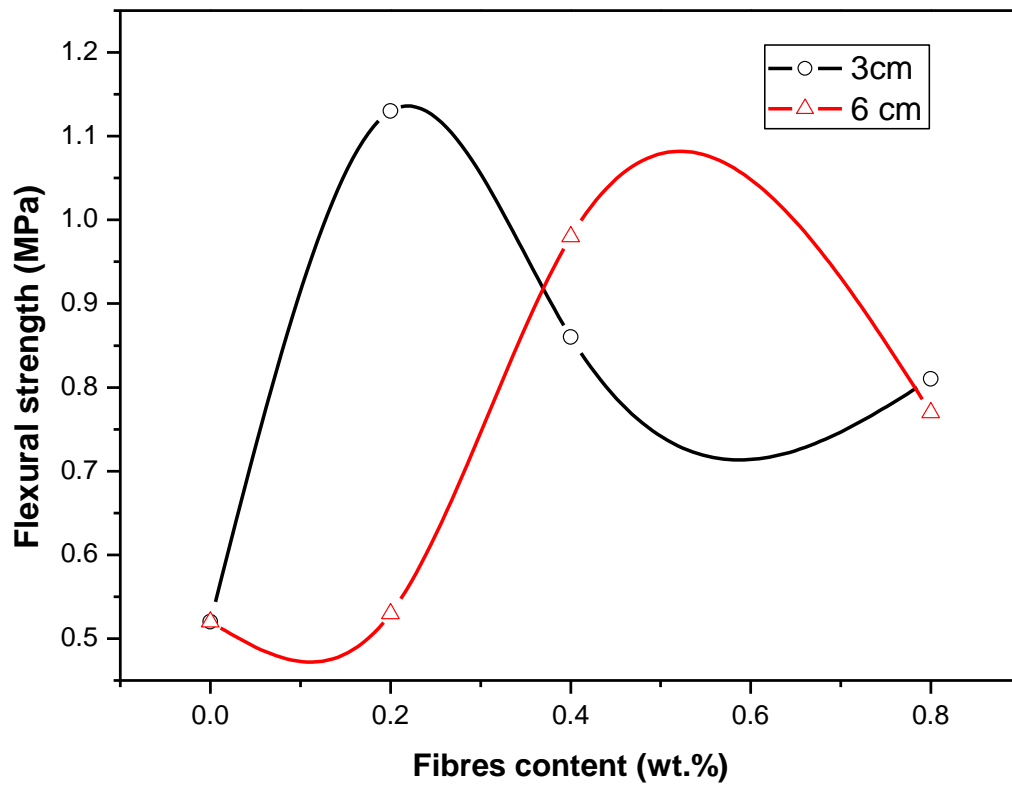


Fig. 14